12. S. Kambhampati, P. Eggleton, in *Termites: Evolution, Sociality, Symbioses, Ecology*, T. Abe, D. E. Bignell, M. Higashi, Eds. (Kluwer Academic, Dordrecht, Netherlands, 2000), pp. 1–24.
13. J. Korb, D. K. Aanen, *Behav. Ecol. Sociobiol.* **53**, 65 (2003).
14. H. H. de Fine Licht, A. Andersen, D. K. Aanen, *Mycol. Res.* **109**, 314 (2005).
15. D. K. Aanen *et al.*, *BMC Evol. Biol.* **7**, 115 (2007).
16. H. H. de Fine Licht, J. J. Boomsma, D. K. Aanen, *Mol. Ecol.* **15**, 3131 (2006).
17. K. R. Foster, T. Wenseleers, *J. Evol. Biol.* **19**, 1283 (2006).
18. S. A. Frank, *Am. Nat.* **150**, S80 (1997).
19. Materials and methods are available as supporting material on *Science* Online.
20. H. Katoh, T. Miura, K. Maekawa, N. Shinzato, T. Matsumoto, *Mol. Ecol.* **11**, 1565 (2002).
21. D. K. Aanen, *Biol. Lett.* **2**, 209 (2006).
22. R. H. Leuthold, S. Badertscher, H. Imboden, *Insect Soc.* **36**, 328 (1989).
23. J. J. Worrall, *Mycologia* **89**, 24 (1997).
24. M. Chamberlain, D. S. Ingram, in *Advances in Botanical Research Incorporating Advances in Plant Pathology* (Academic Press, London, 1997), vol. 24, pp. 71–87.
25. M. Poulsen, J. J. Boomsma, *Science* **307**, 741 (2005).
26. C. O. Micali, M. L. Smith, *Fungal Genet. Biol.* **38**, 209 (2003).
27. I. H. Chapela, S. A. Rehner, T. R. Schultz, U. G. Mueller, *Science* **266**, 1691 (1994).
28. U. G. Mueller, S. A. Rehner, T. R. Schultz, *Science* **281**, 2034 (1998).
29. T. R. Schultz, S. G. Brady, *Proc. Natl. Acad. Sci. U.S.A.* **105**, 5435 (2008).
30. T. G. Wood, R. J. Thomas, in *Insect-Fungus Interactions*, N. Wilding, N. M. Collins, P. M. Hammond, J. F. Webber, Eds. (Academic Press, London, 1989), pp. 69–92.
31. J. J. Bull, W. R. Rice, *J. Theor. Biol.* **149**, 63 (1991).
32. E. T. Kiers, R. A. Rousseau, S. A. West, R. F. Denison, *Nature* **425**, 78 (2003).
33. J. D. Bever, S. C. Richardson, B. M. Lawrence, J. Holmes, M. Watson, *Ecol. Lett.* **12**, 13 (2009).
34. N. Knowlton, F. Rohwer, *Am. Nat.* **162**, S51 (2003).
35. J. Maynard Smith, E. Szathmáry, *The Major Transitions in Evolution* (Oxford Univ. Press, Oxford, 1995).
36. We were supported by fellowships from the Netherlands Organization for Scientific Research—Vidi (D.K.A.); the C. T. de Wit Graduate School for Production Ecology and Resource Conservation, Wageningen University, Netherlands (D.K.A.); the Danish National Research Foundation (J.J.B.); and the Danish Natural Science Research Council—STENO (D.K.A.). We thank A. de Visser for help with statistical analyses and for comments on an earlier version of the manuscript, T. Nobre for comments, B. Nieuwenhuis for help with the figures, and the Forestry and Agricultural Biotechnology Institute (FABI) team led by M. Wingfield at the University of Pretoria for providing facilities during field and laboratory work.

Supporting Online Material

www.sciencemag.org/cgi/content/full/326/5956/1103/DC1
Materials and Methods
SOM Text
Figs. S1 to S4
Tables S1 to S4
References

12 March 2009; accepted 25 September 2009
10.1126/science.1173462

Epicontinental Seas Versus Open-Ocean Settings: The Kinetics of Mass Extinction and Origination

Arnold I. Miller[1]* and Michael Foote[2]

Environmental perturbations during mass extinctions were likely manifested differently in epicontinental seas than in open-ocean–facing habitats of comparable depth. Here, we present a dissection of origination and extinction in epicontinental seas versus open-ocean–facing coastal regions in the Permian through Cretaceous periods, an interval through which both settings are well represented in the fossil record. Results demonstrate that extinction rates were significantly higher in open-ocean settings than in epicontinental seas during major mass extinctions but not at other times and that origination rates were significantly higher in open-ocean settings for a protracted interval from the Late Jurassic through the Late Cretaceous. These patterns are manifested even when other paleogeographic and environmental variables are held fixed, indicating that epicontinental seas and open-ocean–facing coastlines carry distinct macroevolutionary signatures.

Throughout the global history of Phanerozoic marine life, patterns of diversification and extinction varied substantially among different regions such as paleocontinents (*1*–*4*) and latitudinal belts (*5*). However, the primary geographic and environmental dichotomy recognized among ancient shallow-marine settings is the distinction between epicontinental seas, which covered broad regions of ancient continents during much of the Paleozoic era but began to wane thereafter, and open-ocean–facing coastlines, which became increasingly important through the Mesozoic and Cenozoic eras and rim present-day continents (*6*, *7*). Because they extended over unusually broad areas with water depths typically less than 100 m, epicontinental seas were likely characterized by sluggish circulation in comparison to coastal settings of comparable depths that faced the open ocean (*8*, *9*), and this may have had important ramifications for taxonomic origination and extinction (*6*, *10*). Potential mass extinction agents were probably manifested differently in the two settings. In epicontinental seas, for example, drops in sea level would have been more lethal because of the rapid subaerial exposure of unusually large expanses of shallow seafloor (*11*, *12*), and biotas there may also have been more susceptible to bottom-water anoxia because of relatively poor circulation and enhanced stratification (*13*). By contrast, shallow open-ocean–facing settings may have been affected more profoundly in cases where waterborne lethal effects emanated from point sources, such as impacts or volcanic events, the propagation of which may have been inhibited in epicontinental seas because of sluggish circulation.

Here, we contrast the kinetics of extinction and origination in epicontinental seas versus shallow ocean-facing settings during the Permian through the Cretaceous periods, an interval through which both settings are well represented in the fossil and sedimentary records. Global occurrences of marine genera were extracted from the Paleobiology Database [PaleoDB (*14*)] for a set of stage-level stratigraphic units that span the study interval. We used global paleogeographic maps (e.g., fig. S1) to demarcate the boundaries of epicontinental seas for each stage (*15*), and we mapped individual occurrences of marine genera in each stage with respect to these two settings on the basis of their paleogeographic locations. These, in turn, were used to parse the roster of 7868 genera into those with affinities for either epicontinental seas or ocean-facing settings in cases where a statistical preponderance of occurrences for a given genus was located in one regime or the other (*15*, *16*). In all, 3432 genera were assignable on this basis, and, of these, 3418 had first and last appearances that were stratigraphically resolvable to the stage level. Patterns of extinction and origination were then compared stage by stage through the study interval for genera with affinities for each of the two regimes, on the basis of their first and last appearances as depicted in the PaleoDB.

Comparative per capita extinction rates (*17*) through the study interval (Fig. 1A) document a striking pattern. Whereas there was virtually no difference in average extinction intensity between the two regimes, open-ocean–facing settings exhibited significantly higher extinction rates during the three most profound mass extinctions in the study interval: the end-Permian, end-Triassic, and end-Cretaceous events. This suggests that ocean-facing settings were more susceptible to the agents of extinction in these events.

In contrast, the penultimate stage of the Permian, the Guadalupian, exhibited a significantly higher extinction rate among genera in epicontinental seas than in open-ocean settings. This difference from the subsequent end-Permian event and the two other major extinctions does not demonstrate conclusively that it was caused by a mechanism unique to that interval. Nevertheless, sea-level regression has been implicated in the Guadalupian extinctions because of the loss of major shallow-water provinces (*12*), and its relation to the suite of catastrophic mechanisms

[1]Department of Geology, University of Cincinnati, Post Office Box 210013, Cincinnati, OH 45221, USA. [2]Department of the Geophysical Sciences, University of Chicago, 5734 South Ellis Avenue, Chicago, IL 60637, USA.

*To whom correspondence should be addressed. E-mail: arnold.miller@uc.edu

potentially implicated in the subsequent end-Permian event remains in question (*18*).

Per capita origination rate trajectories (Fig. 1B) generally exhibited more volatility than extinction rate trajectories, with numerous instances in which origination rates for a given stage were higher in one regime or the other and with no consistent pattern before the Kimmeridgian, the penultimate stage of the Jurassic. However, open-ocean settings thereafter exhibited significantly higher origination rates than epicontinental seas for nearly all of the remaining stages of the Mesozoic era.

Of potential relevance to this shift in origination rates, the mean geographic ranges of open-ocean–facing genera declined in the Late Jurassic (Fig. 1C) (*15*). Because reduced geographic range enhances the spatial isolation of taxa, such taxa may exhibit higher origination rates (*19*), and this may explain the increased origination rate among open-ocean–facing genera at that time. Despite the decline in geographic range, however, open-ocean genera maintained larger ranges through most of the Cretaceous than their epicontinental-sea counterparts. Furthermore, an increase in geographic

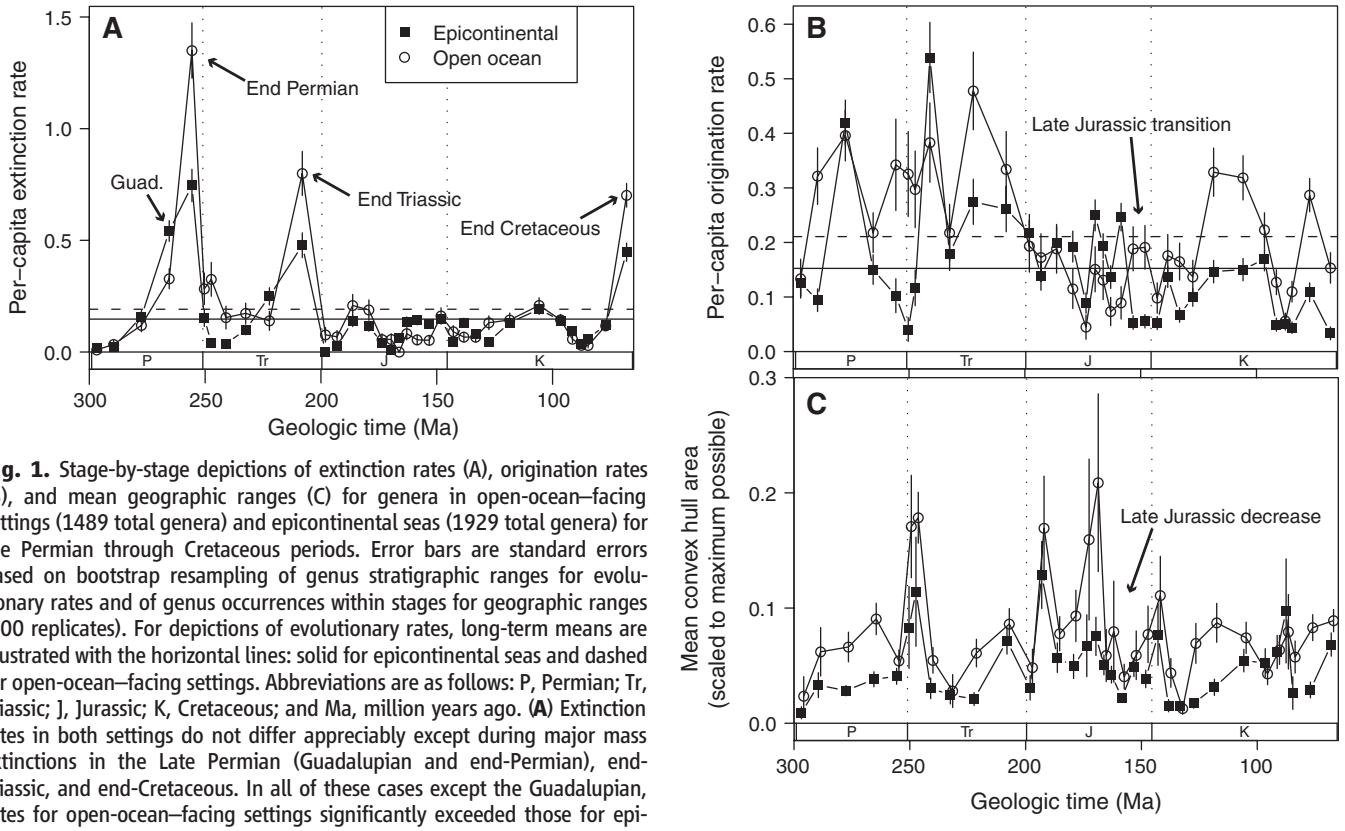

Fig. 1. Stage-by-stage depictions of extinction rates (A), origination rates (B), and mean geographic ranges (C) for genera in open-ocean–facing settings (1489 total genera) and epicontinental seas (1929 total genera) for the Permian through Cretaceous periods. Error bars are standard errors based on bootstrap resampling of genus stratigraphic ranges for evolutionary rates and of genus occurrences within stages for geographic ranges (500 replicates). For depictions of evolutionary rates, long-term means are illustrated with the horizontal lines: solid for epicontinental seas and dashed for open-ocean–facing settings. Abbreviations are as follows: P, Permian; Tr, Triassic; J, Jurassic; K, Cretaceous; and Ma, million years ago. (**A**) Extinction rates in both settings do not differ appreciably except during major mass extinctions in the Late Permian (Guadalupian and end-Permian), end-Triassic, and end-Cretaceous. In all of these cases except the Guadalupian, rates for open-ocean–facing settings significantly exceeded those for epicontinental seas. (**B**) Origination rates were generally more volatile than extinction rates, with no consistent difference between the two regimes until the Kimmeridgian; thereafter, open-ocean rates exceeded those for epicontinental seas in nearly every stage. (**C**) Mean geographic ranges of genera, which are based on convex-hull area scaled to the maximum possible (*15*), exhibit a volatile pattern through the study interval but nevertheless depict a significant downward trend for open-ocean–facing settings through the Late Jurassic.

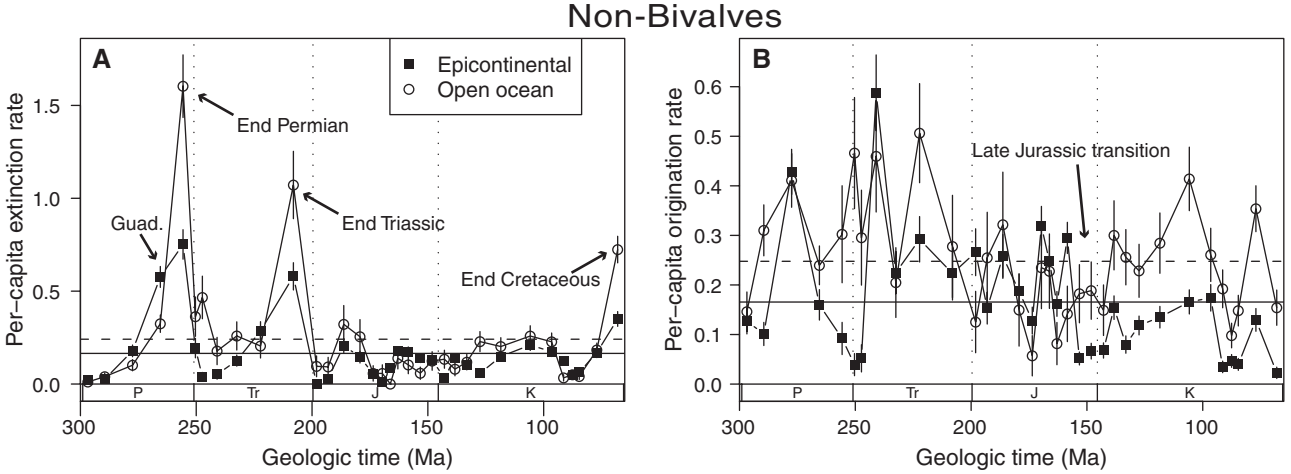

Fig. 2. Stage-by-stage depictions of extinction rates (**A**) and origination rates (**B**) for non-bivalve genera in open-ocean–facing settings (1088 total genera) and epicontinental seas (1617 total genera) for the Permian through Cretaceous periods. Salient features observed in Fig. 1, including elevated open-ocean extinction rates during major mass extinctions and higher open-ocean origination rates from the Kimmeridgian through the remainder of the study interval, are maintained, despite the exclusion of bivalves from the analysis.

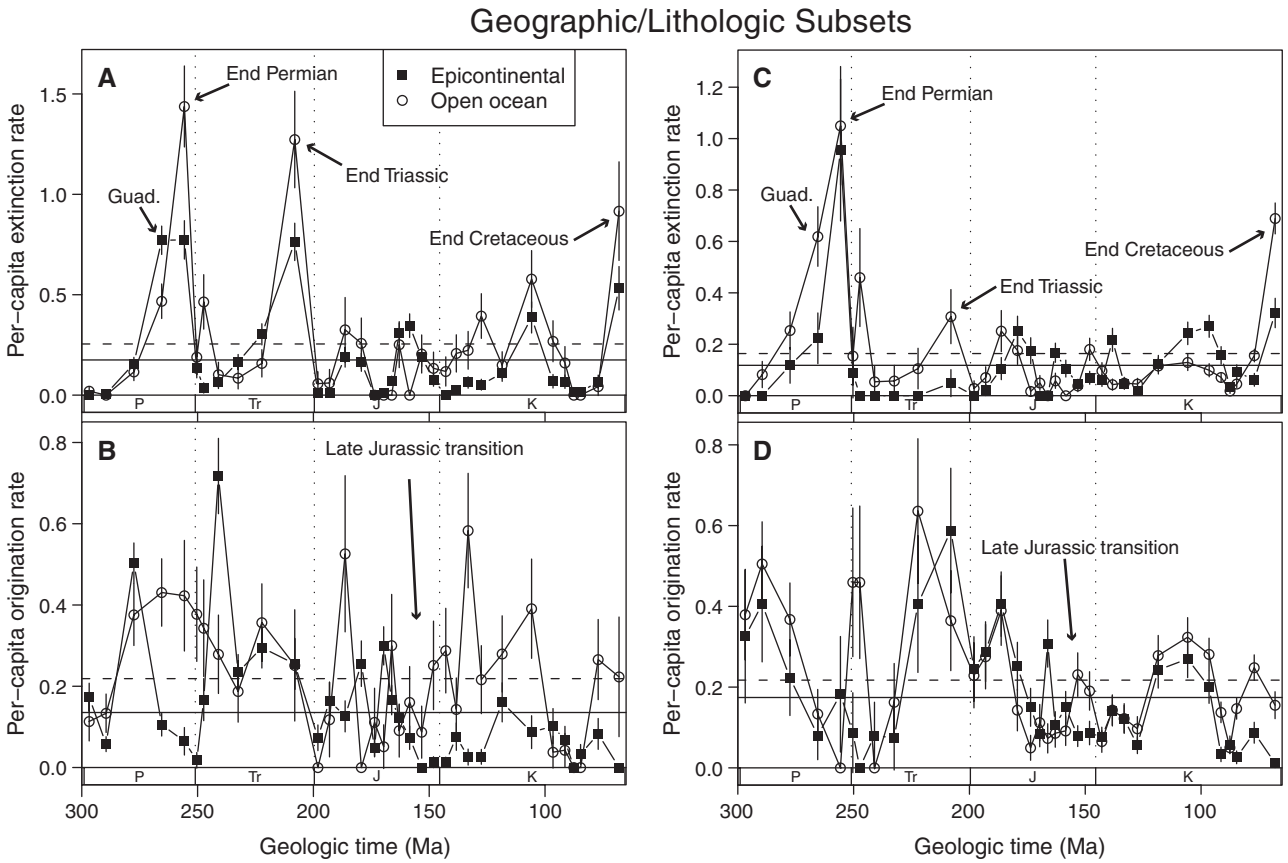

Fig. 3. Stage-by-stage depictions of extinction rates and origination rates for genera in open-ocean–facing settings and epicontinental seas for the Permian through Cretaceous periods for subsets of the data limited to tropical carbonate regimes (**A** and **B**) (822 total genera for epicontinental seas and 508 for open-ocean–facing settings), and nontropical clastic regimes (**C** and **D**) (513 total genera for epicontinental seas and 792 for open-ocean–facing settings) (*15*). As in Fig. 2, salient features observed in Fig. 1 are maintained for tropical carbonate regimes, but extinction characteristics for nontropical clastic regimes are altered for the Late Permian, perhaps reflecting the relative paucity of data from these regimes for the Permian. This exception notwithstanding, the general maintenance of the differences observed in Fig. 1 between epicontinental seas and open-ocean–facing settings indicates that it transcends paleolatitude and sedimentary regime.

range of open-ocean genera through the late Early Cretaceous appears to coincide with an increase, rather than a decrease, in origination rate.

Although a decline in geographic range does not explain the shift in origination rates among open-ocean genera, this decline is intriguing in its own right because an increase in region-to-region faunal differentiation among marine biotas has recently been documented through the Jurassic (*20*). As the northern Atlantic Ocean opened in the Jurassic (*21*), the distance between its western and eastern margins may have separated enough that ocean-facing biotas in these two coastal regions became effectively isolated.

Bivalve molluscs compose a large percentage of the genera contained in most Mesozoic stratigraphic bins when compared with other higher taxa, so we tested whether the patterns documented here were driven by properties inherent to bivalves or instead transcended higher taxonomic membership by using a data set from which all bivalves had been removed. The principal patterns illustrated in Fig. 1, A and B, remained unchanged (Fig. 2).

Most epicontinental seas throughout the Phanerozoic—particularly in the Paleozoic—were in tropical settings (i.e., less than 30° latitude) and dominated by carbonate sedimentation (*6*, *7*), whereas open-ocean–facing coasts—particularly in the Mesozoic and Cenozoic—predominated in nontropical settings characterized by terrigenous clastic sedimentation. Because latitude and the nature of sedimentation are known to have substantially affected Phanerozoic diversity (*16*, *22*, *23*), this raises the prospect that our results might reflect these other, correlated factors. We therefore analyzed data sets limited first to tropical, carbonate settings and then to nontropical, clastic settings. In both cases, most major features illustrated in Fig. 1 were preserved (Fig. 3) with a few exceptions: Most notably, nontropical clastic settings did not exhibit a significantly higher Guadalupian epicontinental-sea extinction rate, and they exhibited only a marginally higher open-ocean rate for the Lopingian (end-Permian; Fig. 3C). This likely relates to a paucity of available data, reflecting the sedimentary and fossil records for that interval: Nontropical clastic data for the Guadalupian and Lopingian included substantially fewer genera, with concomitantly higher uncertainties in rate estimates, than coeval data from tropical-carbonate milieus. This is especially true for epicontinental genera: In the Guadalupian, only 19 are sampled in nontropical clastic milieus, compared with 264 in tropical carbonates; in the Lopingian the corresponding numbers are 24 and 113. Overall, however, these results show that most of our findings were not affected or caused by overprints of paleolatitude or substrate type.

Our results therefore provide evidence of significant differences in the kinetics of mass extinction and origination in epicontinental seas versus shallow, open-ocean–facing settings during the Permian through Cretaceous periods. Because there was a secular transition through the Phanerozoic in the relative spatial extent of these two regimes, there may have been parallel transitions in the relative importance of causes of extinction and origination that acted preferentially in one regime or the other.

References and Notes

1. D. Jablonski, *Science* **279**, 1327 (1998).
2. A. Z. Krug, M. E. Patzkowsky, *Paleobiology* **33**, 435 (2007).
3. A. I. Miller, *Paleobiology* **23**, 410 (1997).
4. A. I. Miller, *Geobios Mem. Spec.* **20**, 397 (1997).
5. A. Z. Krug, D. Jablonski, J. W. Valentine, K. Roy, *Astrobiology* **9**, 113 (2009).
6. S. E. Peters, *Nature* **454**, 626 (2008).
7. L. J. Walker, B. H. Wilkinson, L. C. Ivany, *J. Geol.* **110**, 75 (2002).

8. R. Slingerland, *Sedimentology* **33**, 487 (1986).
9. M. R. Wells *et al.*, *J. Sediment. Res.* **77**, 843 (2007).
10. P. A. Allison, M. R. Wells, *Palaios* **21**, 513 (2006).
11. P. M. Sheehan, *Annu. Rev. Earth Planet. Sci.* **29**, 331 (2001).
12. S. Z. Shen, G. R. Shi, *Paleobiology* **28**, 449 (2002).
13. S. E. Peters, *Paleobiology* **33**, 165 (2007).
14. http://paleodb.org/
15. Materials and methods are available as supporting material on *Science* Online.
16. M. Foote, *Paleobiology* **32**, 345 (2006).
17. M. Foote, *Paleobiology* **26** (suppl. 1), 74 (2000).
18. M. E. Clapham, S. Z. Shen, D. J. Bottjer, *Paleobiology* **35**, 32 (2009).
19. D. Jablonski, K. Roy, *Proc. R. Soc. London Ser. B* **270**, 401 (2003).
20. A. I. Miller *et al.*, *Paleobiology* **35**, 612 (2009).
21. K. O. Emery, E. Uchupi, *The Geology of the Atlantic Ocean* (Springer-Verlag, Berlin, 1984).
22. W. Kiessling, M. Aberhan, *Paleobiology* **33**, 414 (2007).
23. A. I. Miller, S. R. Connolly, *Paleobiology* **27**, 768 (2001).
24. We thank D. Buick, W. Kiessling, S. Kolbe, A. Lagomarcino, and J. Wittmer for discussions; two anonymous reviewers for helpful comments; A. Lagomarcino for assistance in drafting figures; and NASA (program in Exobiology) and NSF (programs in Biocomplexity and in Geology and Paleontology) for financial support. This is Paleobiology Database publication no. 102.

Supporting Online Material
www.sciencemag.org/cgi/content/full/326/5956/1106/DC1
Materials and Methods
Figs. S1 to S3
References

3 August 2009; accepted 16 September 2009
10.1126/science.1180061

A Periplasmic Reducing System Protects Single Cysteine Residues from Oxidation

Matthieu Depuydt,[1] Stephen E. Leonard,[2] Didier Vertommen,[1] Katleen Denoncin,[1] Pierre Morsomme,[3] Khadija Wahni,[4,5] Joris Messens,[4,5] Kate S. Carroll,[2] Jean-François Collet[1]*

The thiol group of the amino acid cysteine can be modified to regulate protein activity. The *Escherichia coli* periplasm is an oxidizing environment in which most cysteine residues are involved in disulfide bonds. However, many periplasmic proteins contain single cysteine residues, which are vulnerable to oxidation to sulfenic acids and then irreversibly modified to sulfinic and sulfonic acids. We discovered that DsbG and DsbC, two thioredoxin-related proteins, control the global sulfenic acid content of the periplasm and protect single cysteine residues from oxidation. DsbG interacts with the YbiS protein and, along with DsbC, regulates oxidation of its catalytic cysteine residue. Thus, a potentially widespread mechanism controls sulfenic acid modification in the cellular environment.

Many proteins secreted into the *Escherichia coli* periplasm contain even numbers of cysteines, most of which form disulfide bonds important for protein stability. These disulfides are introduced by the oxidoreductase enzyme DsbA (disulfide bond A), which is reoxidized by DsbB [reviewed in (*1*)]. When proteins require disulfides to be formed between nonconsecutive cysteines, DsbA can introduce incorrect disulfides. These non-native disulfides are corrected by the isomerase DsbC, a V-shaped dimeric protein. Each subunit of DsbC contains a CXXC motif, located within a thioredoxin fold, which is kept reduced by DsbD, a membrane protein that transfers electrons from the cytoplasmic thioredoxin system to the periplasm (*1*).

The periplasm contains another protein that could potentially serve as an isomerase, DsbG (*2*). DsbG shares 26% sequence identity with DsbC and is also a V-shaped dimeric protein, with a thioredoxin fold and a CXXC motif that is kept reduced by DsbD. The structure of DsbG resembles that of DsbC, but the dimensions of the DsbG cleft are larger and its surface is less hydrophobic (*3*). It has thus been predicted that DsbG preferentially interacts with proteins that are folded or partially folded (*3*). However, the substrates of DsbG are not known and its function has remained obscure.

We sought to clearly define the function of DsbG by identifying its substrates. We first used a global proteomics approach to compare the proteome of a *dsbG* mutant strain to that of a wild type but did not find a single protein that was affected by the absence of DsbG (table S1).

To trap DsbG bound to its substrates, we produced the $DsbG_{CXXA}$ mutant, in which an alanine replaces the second cysteine of the CXXC motif. This approach has been used to trap thioredoxin substrates (*4*). $DsbG_{CXXA}$ was purified under denaturing conditions. DsbG and slower migrating bands were present in the purified sample (Fig. 1A). Addition of the reducing agent dithiothreitol (DTT) led to the disappearance of most of these bands and the corresponding increase of DsbG, which suggests that the upper bands corresponded to DsbG bound to unknown proteins.

The complexes were separated by two-dimensional gel electrophoresis (Fig. 1B). Three periplasmic proteins, YbiS, ErfK, and YnhG, were potential substrates of DsbG. The cytosolic proteins Ef-Tu, DnaK, and Fur were also identified but probably represent false positives that react with DsbG during cell lysis. Indeed, Ef-Tu has highly reactive cysteines and has also been found in a complex with DsbA (*5*).

The three periplasmic proteins are homologous proteins belonging to the same family of L,D-transpeptidases, which catalyze the cross-linking of peptidoglycan for cell wall synthesis (fig. S1). Because they possess a sole cysteine, essential for activity (*6*), these proteins are not likely in need of a disulfide isomerase but rather of a reductase to rescue their cysteine from oxidation within the oxidizing periplasm. To investigate this further, we studied the interaction between

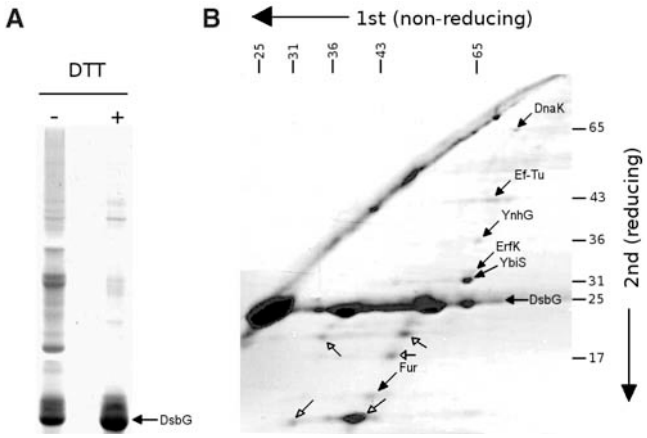

Fig. 1. Identification of DsbG substrates. **(A)** SDS-PAGE analysis of purified $DsbG_{CXXA}$. **(B)** Separation of the complexes in a second reducing dimension. Proteins were identified by mass spectrometry. Open arrows correspond to smaller versions of DsbG resulting from proteolysis.

[1]de Duve Institute, Université catholique de Louvain, B-1200 Brussels, Belgium. [2]Life Sciences Institute, University of Michigan, Ann Arbor, MI 48109–1048, USA. [3]Institut des Sciences de la Vie, Université catholique de Louvain, B-1348 Louvain-la-Neuve, Belgium. [4]Department of Molecular and Cellular Interactions, Vlaams Instituut voor Biotechnologie (VIB), Vrije Universiteit Brussel, B-1050 Brussels, Belgium. [5]Structural Biology Brussels, Vrije Universiteit Brussel, B-1050 Brussels, Belgium.

*To whom correspondence should be addressed. E-mail: jfcollet@uclouvain.be